Trends in continental temperature and humidity directly linked to ocean warming

SI Appendix
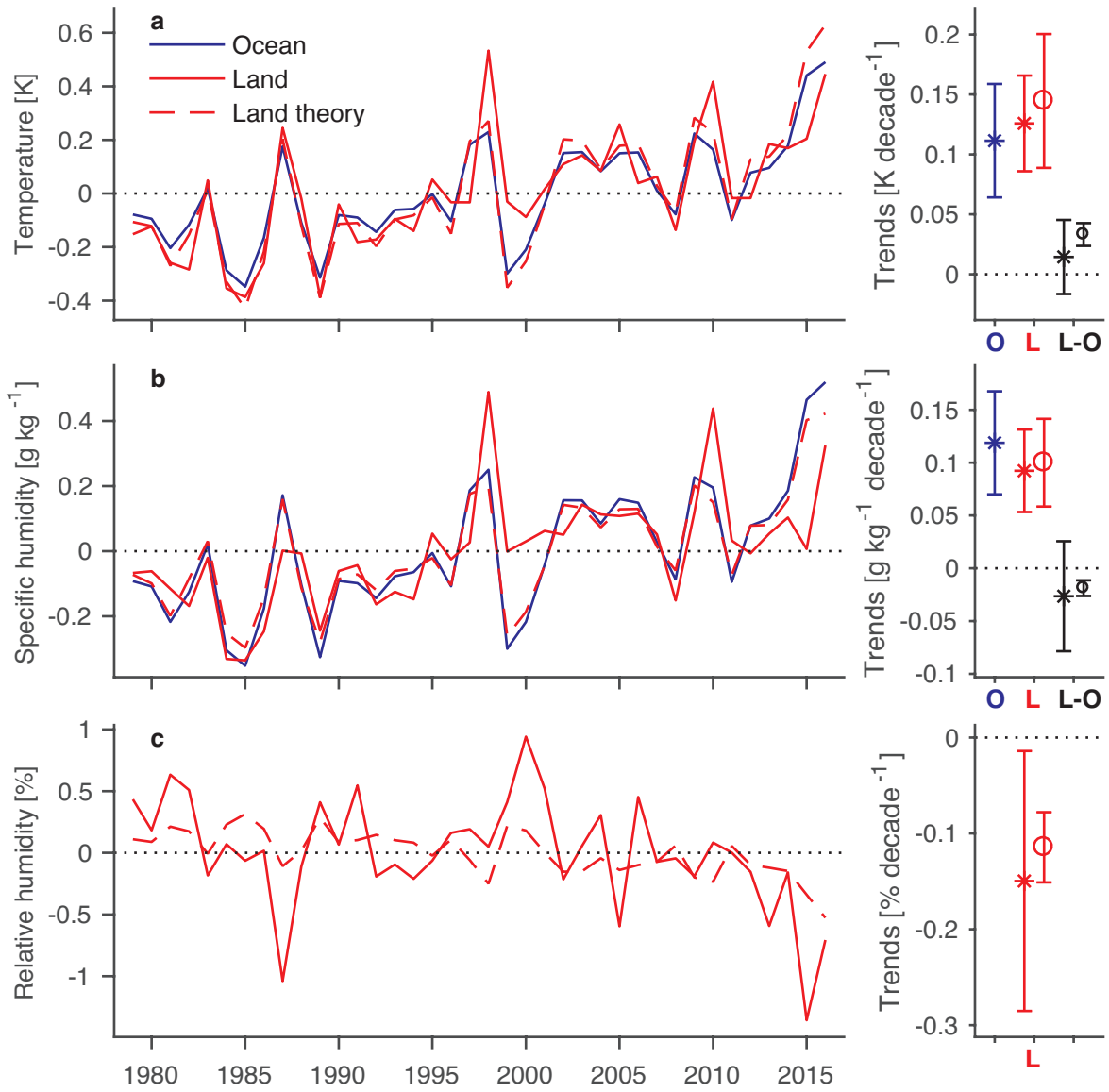
Michael P. Byrne & Paul A. O'Gorman

1

Figure S1: As in Figure 1, but here showing the surface-air (a) temperature, (b) specific humidity and (c) relative humidity anomalies averaged over 20°S to 20°N.
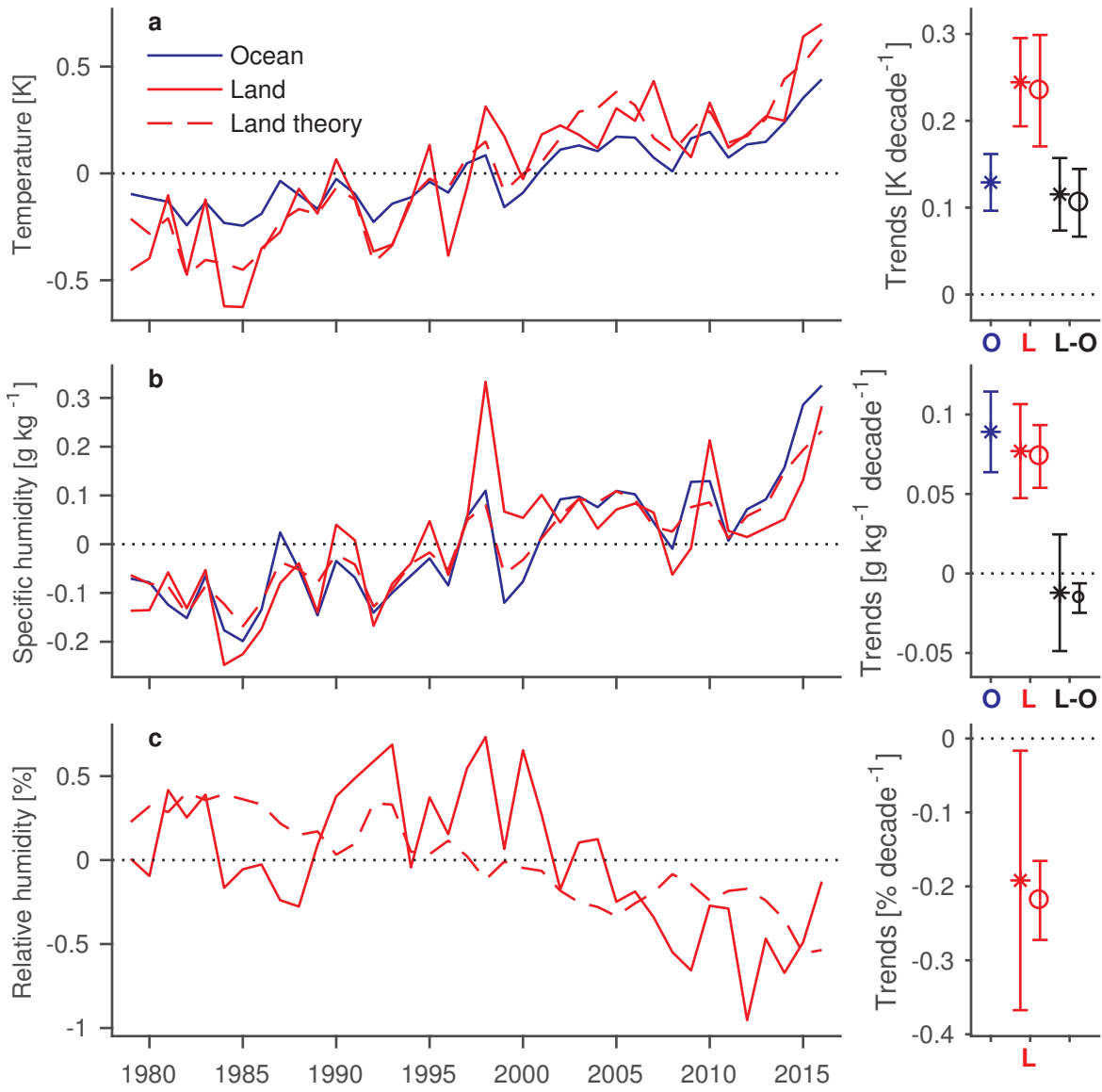
Figure S2: As in Figure 1, but here showing the surface-air (a) temperature, (b) specific humidity and (c) relative humidity anomalies averaged over 60°S to 80°N.
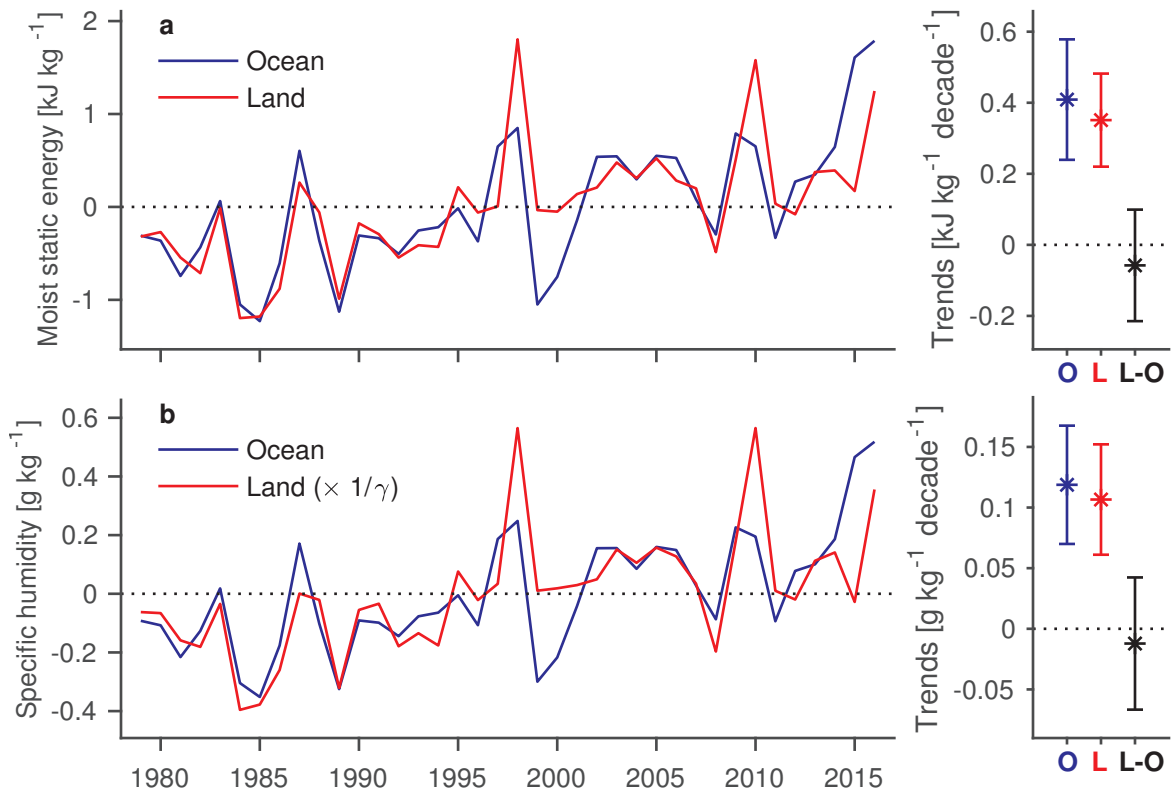
Figure S3: As in Figure 2, but here showing the surface-air (a) moist static energy and (b) specific humidity anomalies averaged over 20°S to 20°N. The land specific humidity anomalies have been re-scaled by a factor $1/\gamma$ so that equal trends over land and ocean correspond to the atmospheric moisture constraint holding (see equation [2]). The average of γ over land gridboxes between 20°S and 20°N is 0.83.

Figure S4: As in Figure 2, but here showing the surface-air (a) moist static energy and (b) specific humidity anomalies averaged over 60°S to 80°N. The land specific humidity anomalies have been re-scaled by a factor $1/\gamma$ so that equal trends over land and ocean correspond to the atmospheric moisture constraint holding (see equation [2]). The average of γ over land gridboxes between 60°S and 80°N is 0.71.
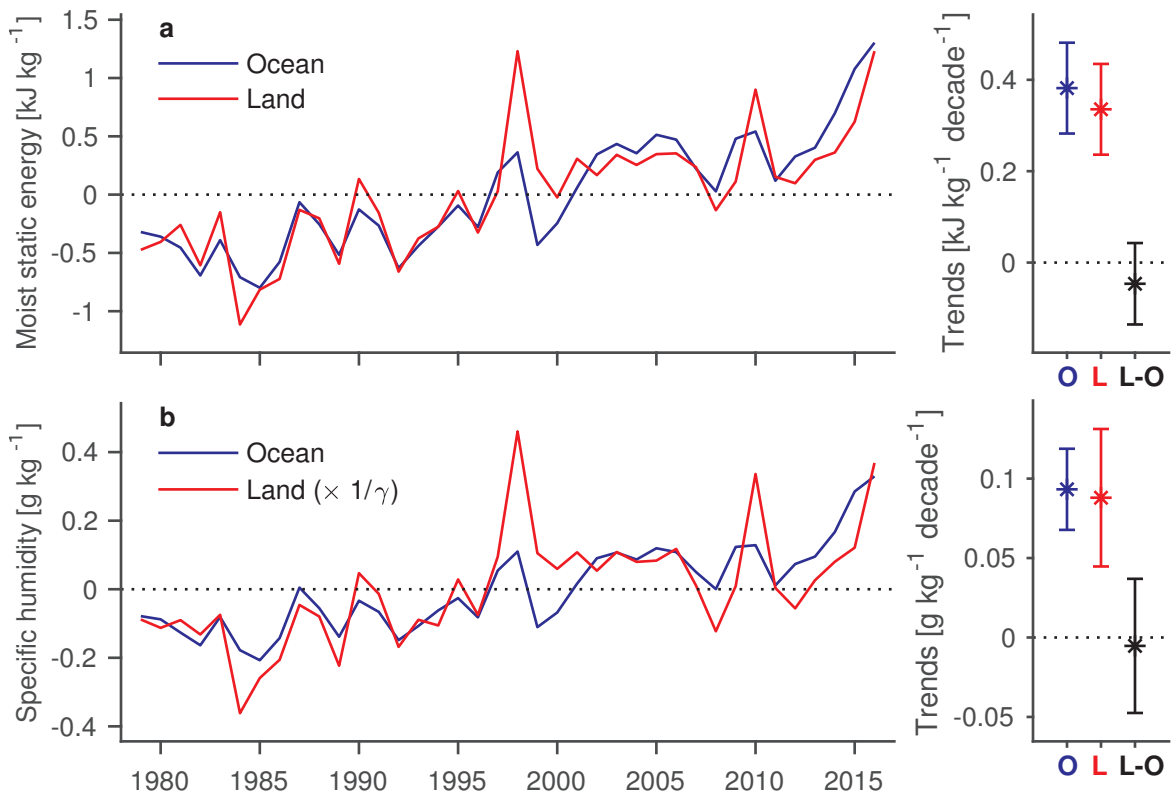
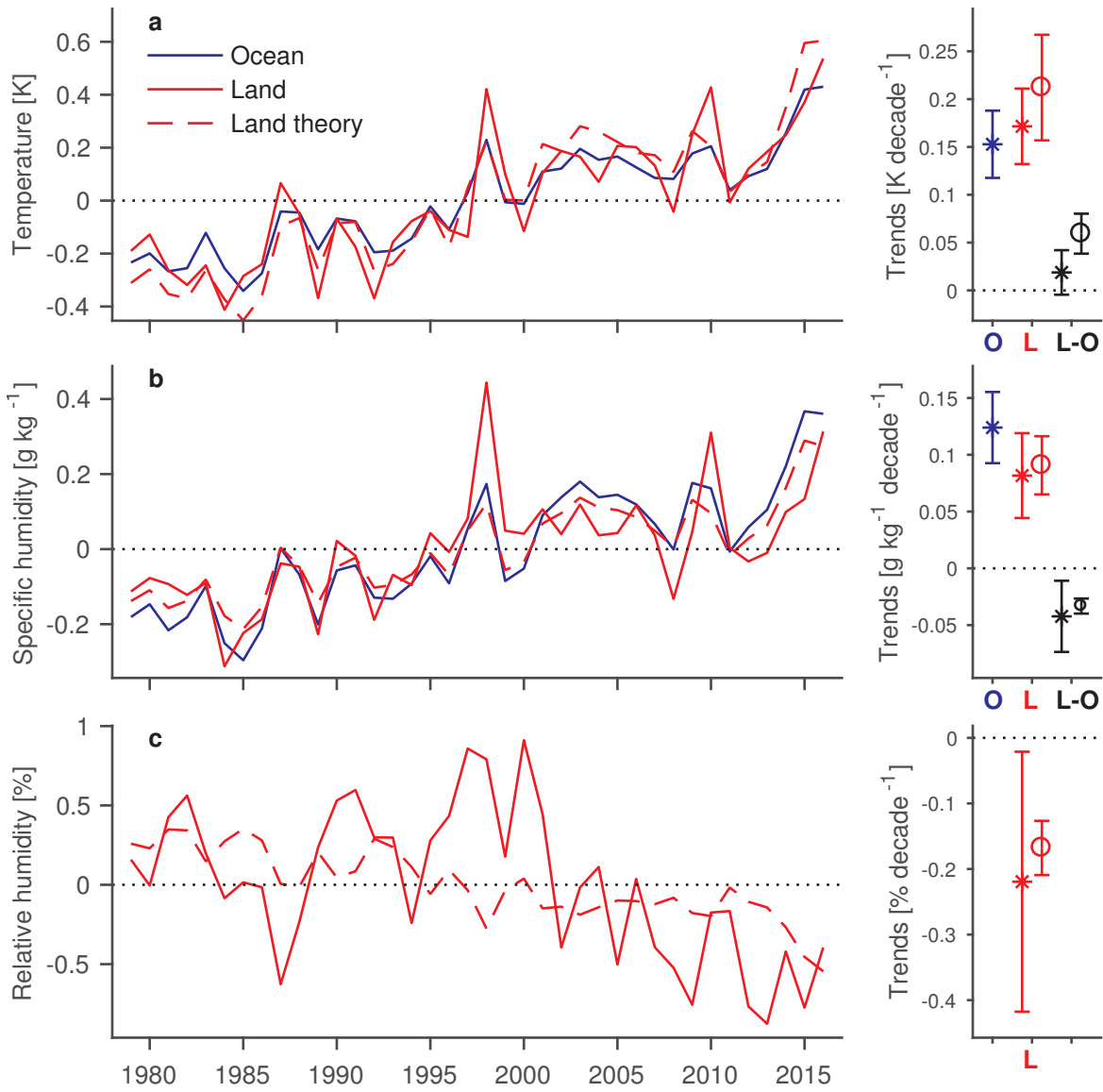Figure S5: As in Figure 1 but here using HadSST3 data for ocean temperature anomalies, to estimate the ocean specific humidity anomalies assuming climatological relative humidity, and as an input to the theory.
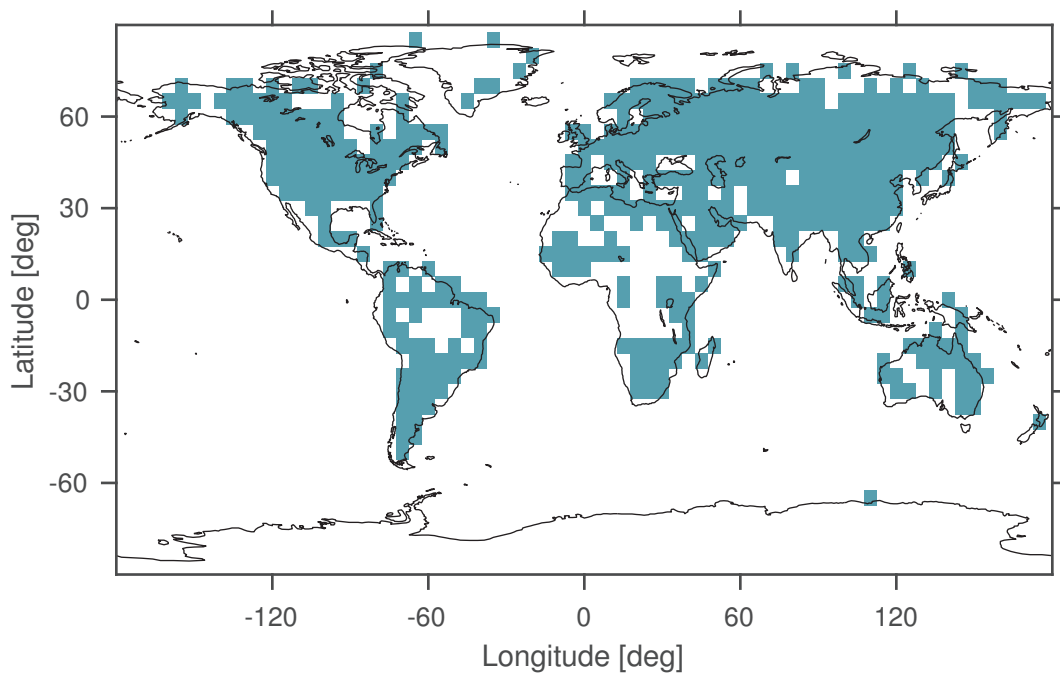
Figure S6: Shading indicates the land gridboxes from the HadISDH dataset that have greater than 50% temporal coverage during 1979-2016 (these are the gridboxes we use to calculate the land anomaly timeseries and trends).
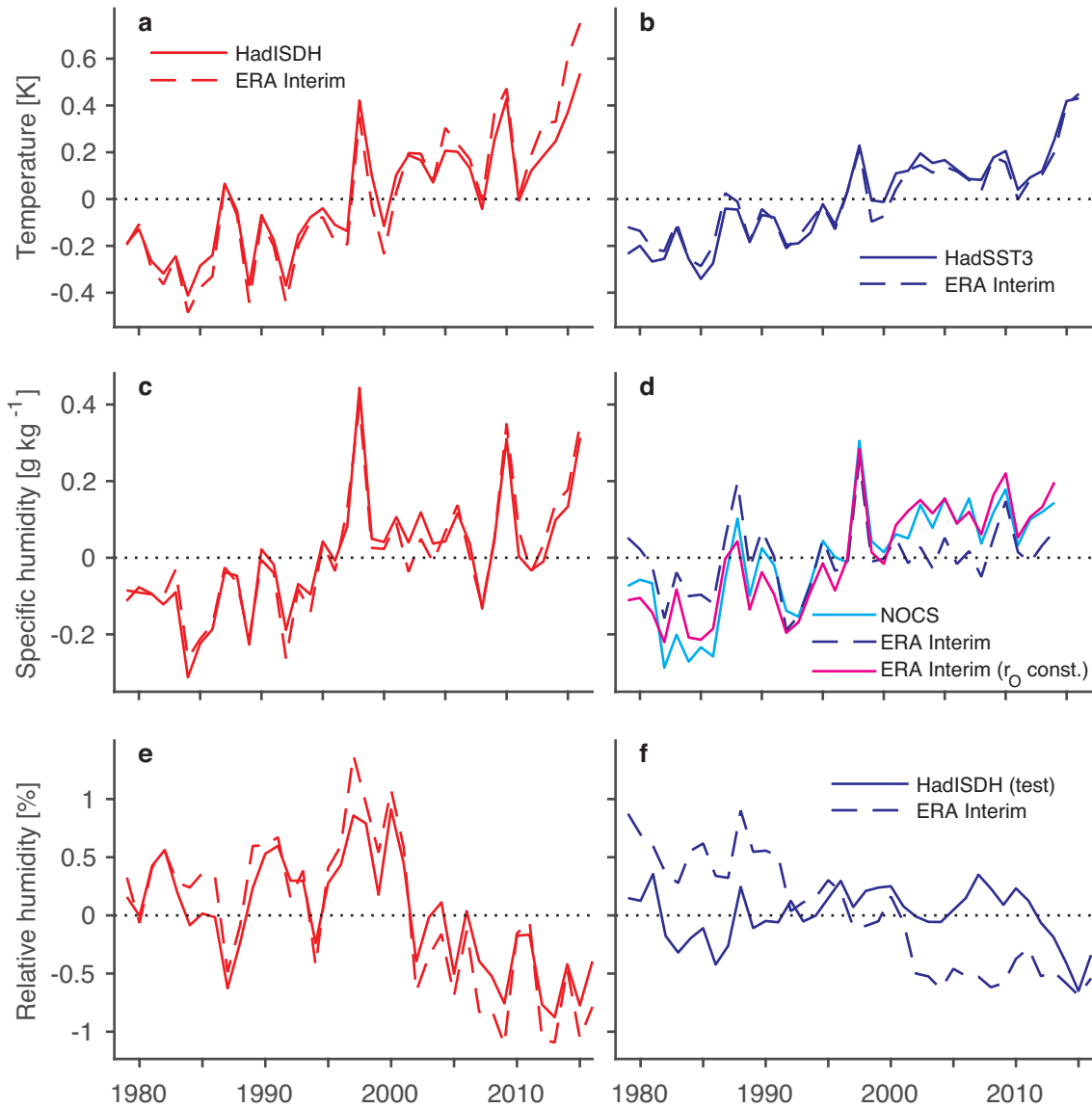
Figure S7: Annual anomalies in (a) land temperature, (b) ocean temperature, (c) land specific humidity, (d) ocean specific humidity, (e) land relative humidity, and (f) ocean relative humidity from observations (solid red, blue and cyan lines) and the ERA-Interim reanalysis (dashed red and blue lines). All values shown are for surface-air quantities except for HadSST3. The magenta line in (d) shows the ocean specific humidity anomalies from ERA Interim calculated assuming a constant climatological relative humidity. All anomalies have been averaged from 40°S to 40°N. ERA-Interim data in this figure are subsampled to the observations as described in the Methods.

Timeseries	20°S to 20°N	40°S to 40°N	60°S to 80°N
δT_{L} (HadISDH)	0.13 ± 0.04	0.17 ± 0.04	0.24 ± 0.05
δT_{L} (theory)	0.14 ± 0.06	0.18 ± 0.05	0.23 ± 0.06
δT_{O} (ERA)	0.11 ± 0.05	0.12 ± 0.04	0.13 ± 0.03
$\delta T_{\mathrm{L}} - \delta T_{\mathrm{O}}$	0.01 ± 0.04	0.05 ± 0.02	0.12 ± 0.04
$\delta T_{\mathrm{L}} - \delta T_{\mathrm{O}}$ (theory)	0.03 ± 0.01	0.07 ± 0.02	0.11 ± 0.04
δq_{L} (HadISDH)	0.09 ± 0.04	0.08 ± 0.04	0.08 ± 0.03
δq_{L} (theory)	0.10 ± 0.04	0.08 ± 0.03	0.07 ± 0.02
δq_{O} (ERA, r_{O} const.)	0.12 ± 0.05	0.11 ± 0.03	0.09 ± 0.03
$\delta q_{\mathrm{L}} - \delta q_{\mathrm{O}}$	-0.03 ± 0.05	-0.03 ± 0.04	-0.01 ± 0.04
$\delta q_{\mathrm{L}} - \delta q_{\mathrm{O}}$ (theory)	-0.02 ± 0.01	-0.03 ± 0.01	-0.02 ± 0.01
δr_{L} (HadISDH)	-0.15 ± 0.14	-0.22 ± 0.20	-0.19 ± 0.18
δr_{L} (theory)	-0.11 ± 0.04	-0.19 ± 0.05	-0.22 ± 0.05

Table S1: **Performance of the simple theory:** Trends in temperature, specific humidity and relative humidity over land (L) and ocean (O) averaged over the specified latitudinal bands and corresponding to the timeseries and trends plotted in Figures 1, S1 and S2. The ocean specific humidity trend is calculated assuming constant climatological relative humidity, as discussed in Methods. The temperature trends are in units of K per decade, the specific humidity trends are in $\mathrm{g\,kg^{-1}}$ per decade and the relative humidity trends are in units of % per decade. All uncertainties indicate the 90% confidence intervals corrected to account for serial correlation.

Timeseries	20°S to 20°N	40°S to 40°N	60°S to 80°N
δT_{L} (HadISDH)	0.13 ± 0.04	0.17 ± 0.04	0.24 ± 0.05
δT_{L} (ERA, sub.)	0.20 ± 0.06	0.22 ± 0.05	0.28 ± 0.06
δT_{O} (HadSST3)	0.14 ± 0.04	0.15 ± 0.04	0.16 ± 0.04
δT_{O} (ERA, sub.)	0.12 ± 0.04	0.13 ± 0.03	0.14 ± 0.04
δq_{L} (HadISDH)	0.09 ± 0.04	0.08 ± 0.04	0.08 ± 0.03
δq_{L} (ERA, sub.)	0.09 ± 0.04	0.09 ± 0.04	0.08 ± 0.03
δq_{O} (NOCS)	0.09 ± 0.04	0.10 ± 0.03	0.10 ± 0.03
δq_{O} (ERA, sub., r_{O} const.)	0.12 ± 0.04	0.11 ± 0.03	0.10 ± 0.03
δq_{O} (ERA, sub.)	0.03 ± 0.04	0.02 ± 0.03	0.03 ± 0.03
δr_{L} (HadISDH)	-0.15 ± 0.14	-0.22 ± 0.20	-0.19 ± 0.18
δr_{L} (ERA, sub.)	-0.41 ± 0.23	-0.35 ± 0.25	-0.35 ± 0.19
δr_{O} (HadISDH marine [test])	0.04 ± 0.13	-0.02 ± 0.14	-0.06 ± 0.13
δr_{O} (ERA, sub.)	-0.41 ± 0.10	-0.40 ± 0.09	-0.37 ± 0.09

Table S2: **Comparison of ERA-Interim reanalysis with observations over land and ocean:** Trends in temperature, specific humidity and relative humidity over land (L) and ocean (O) averaged over the specified latitudinal bands. All values are for surface-air quantities except for the HadSST3 ocean temperature trends, which are sea-surface temperatures. All trends are calculated over 1979-2016 except for the ocean specific humidity trends, which are all calculated over 1979-2014 so as to be consistent with the NOCS dataset (which has data available only up to 2014). The temperature trends are in units of K per decade, the specific humidity trends are in $\mathrm{g\,kg^{-1}}$ per decade and the relative humidity trends are in units of % per decade. All uncertainties indicate the 90% confidence intervals corrected to account for serial correlation. ERA-Interim data for this table are subsampled to the observations as described in the Methods.